ORIGINAL ARTICLE

(-)-Epigallocatechin-3-gallate provides neuroprotection via AMPK activation against traumatic brain injury in a mouse model

Yinyin Wu[1] · Jing Cui[1]

Abstract

Traumatic brain injury (TBI) is a leading cause of death and disability worldwide. (-)-Epigallocatechin-3-gallate (EGCG) has shown robust neuroprotective effects on various brain injury models in rodents. Herein, we aimed to investigate if EGCG protects against TBI and unravel the underlying mechanisms. A total of 102 mice were used for this study. TBI was induced by controlled cortical impact (CCI). EGCG was given immediately after TBI injury. Neurological functions were accessed by corner test, paw placement, modified neurological severity score, rotarod test, and Morris water maze test. AMPK inhibitor and AMPKα1-knockout mice were used to further study the signaling pathways involved in the observed effects. Our results show that EGCG significantly ameliorated CCI-induced neurological impairment, including spatial learning and memory. EGCG suppressed CCI-induced inflammation and oxidative stress. Furthermore, EGCG downregulated the phosphorylation of IKKα/β, IκBα, and nuclear translocation of NF-κB p65; upregulated AMPK phosphorylation; and altered corresponding changes in the phosphorylation of the downstream target's ribosomal protein S6, AS160, and CaMKKβ. Our data demonstrate that EGCG protects against CCI-induced TBI through the activation of the AMPK pathway in mice, suggesting that EGCG might be a promising therapeutic intervention preventing locomotor and cognitive impairments after TBI.

Keywords (-)-Epigallocatechin-3-gallate · Controlled cortical impact · Neurological function · Inflammation · Oxidative stress · AMPK

Introduction

Traumatic brain injury (TBI) causes long-term disability and death for millions. It remains an enormous societal and economic burden (Maas et al. 2017). Two stages of brain injuries, primary and secondary brain injuries, are classified in TBI (Kaur and Sharma 2018; Pearn et al. 2017; Pushkarna et al. 2010). Of which, primary injury is caused at the time of the initial damage force, including tissue destruction and distortion in the early post-injury period. Secondary injury occurs from hours to days to months after the initial trauma. It is the result of disturbance of brain and systemic physiology following the traumatic event, such as the formation of cerebral edema, intracranial hematoma, depolarization, excitotoxicity, metabolic abnormalities, and disruption of the blood-brain barrier. Since very few can be done to influence the primary injury, traditional treatment strategies mainly focused on the intervention of secondary brain injuries. However, many potential therapeutics that are effective in preventing secondary injuries in TBI animal models have failed in phase III clinical trials (Loane and Faden 2010). One of the important reasons is that the exact secondary injury mechanism of TBI remains unclear (Khan et al. 2018; Liu et al. 2018a).

Epigallocatechin gallate ((-)-epigallocatechin-3-gallate, EGCG), the main catechol component extracted from green tea, has been reported to have a variety of biological activities, such as anti-carcinogenic activity (Lecumberri et al. 2013; Li et al. 2018), lowering blood cholesterol (Ikeda 2008), angiogenesis (Kondo et al. 2002; Tang et al. 2003), anti-oxidation (Ding et al. 2018; Meng et al. 2008; Nagai et al. 2002), and anti-inflammatory (Chu et al. 2017; Tedeschi et al. 2004). EGCG has also been found to be neuroprotective in neurodegenerative diseases including Alzheimer's disease and Parkinson's disease (Ehrnhoefer et al. 2008; Ide et al. 2018).

Yinyin Wu and Jing Cui contributed equally to this work.

✉ Yinyin Wu
wuyinyintree@163.com

[1] The Second People's Hospital of Hefei City, Intersection of Guangde Road and Leshui Road, Yaohai District, Hefei 230011, Anhui, China

Since inflammatory reaction, oxidative stress, and cellular energy metabolism disorders caused by mitochondrial dysfunction are included in the TBI secondary injury, the present study aims to investigate if EGCG exhibits beneficial effects against TBI.

It has been reported that EGCG promotes the production of neural stem cells around injured tissues impaired by a pneumatic controlled injury device (Itoh et al. 2012). Recently, four TBI models are widely used in research: fluid percussion injury (FPI), controlled cortical impact (CCI) injury, weight-drop impact acceleration injury, and blast injury (Xiong et al. 2013). EGCG was also reported to inhibit the production of nitric oxide, which is the indicator of enhanced oxidation in injured brain tissue (Ding et al. 2018). However, no clear underlying mechanisms were documented yet. Mitochondrial dysfunction is an important downstream cascade reaction of TBI (Scheff and Ansari 2017). The mitochondria are involved in intracellular energy metabolism, and 5′ adenosine monophosphate-activated protein kinase (AMPK) is a major sensor of energy metabolism (Harun-Or-Rashid and Inman 2018). In addition, AMPK is an important serine/threonine kinase; the activation of AMPK and its downstream signaling pathways can effectively inhibit inflammatory responses (Briones et al. 2013; Harun-Or-Rashid and Inman 2018). Previous studies suggest that EGCG is an AMPK activator (Briones et al. 2013). Therefore, we hypothesize that EGCG is potent to protect against TBI. The aim of this study is to investigate whether EGCG protects against TBI and elucidate the underlying molecular mechanisms.

Material and methods

Animals

One hundred two male C57BL/6 mice (8 weeks old), AMPKα1$^{flox/flox}$ mice, and Rosa^{Cre-ER} mice were purchased from Nanjing Model Animal Institute (Nanjing, China). All animals were housed and bred with open access to food and water. Animals were maintained at 24 °C ± 1 °C with a standard 12-h light-dark cycle. Deletion of AMPKα1 was induced by tamoxifen injection in AMPKα1$^{flox/flox}$/Rosa^{Cre-ER} mice.

CCI injury procedure and drug administration

CCI was performed as previously described (Liu et al. 2018b). Mice were anesthetized with inhaled 3% isoflurane for induction and 1–2% for maintenance. A 10-mm midline incision was made from the eye level to the neck level to expose the dorsal surface of the skull. Then, a 4-mm burr hole was drilled over the right somatosensory cortex between bregma and lambda suture lines, without hurting the dura intact. CCI injury was introduced by an impact velocity of 1.5 m/s,

deformation depth of 1.5 mm, and dwell time of 100 ms, which was created by the Impact One™ Stereotaxic CCI Instrument (Leica Microsystems; Germany) outfitted with a 2-mm diameter piston. After CCI, the dura was intact, and a bone wax was used to seal the cranial opening. Sham animals received the same operation without CCI injury. EGCG (0.2%, w/v (%), dissolved in drinking water, which was verified effective in our pilot study (data not shown)) was provided immediately after CCI injury and accessible till the endpoint experiment. Sham-operated and controlled CCI animals received normal drinking water. To compare EGCG effects with 5-aminoimidazole-4-carboxamide ribonucleotide (AICAR) or metformin on AMPK phosphorylation, 500 mg/kg AICAR, 250 mg/kg metformin, or the combination was *i.p.* injected twice at 5 min and 24 after CCI injury (Hill et al. 2016). Experimental procedures were shown in schematic Fig. 1. The neurological severity score was assessed at 1, 3, 7, and 14 days after CCI procedure; Morris water maze test was then performed from day 14 to day 18 post-injury. After a probe trial, all animals were euthanized. The rest of the behavioral tests were performed 24 h after CCI. Mice were euthanized after the behavioral tests were done to collect blood or brain samples for further analysis. All animal procedures were in accordance with the Guide for the Care and Use of Laboratory Animals (8th edition, NIH) and approved by The Second People's Hospital of Hefei City.
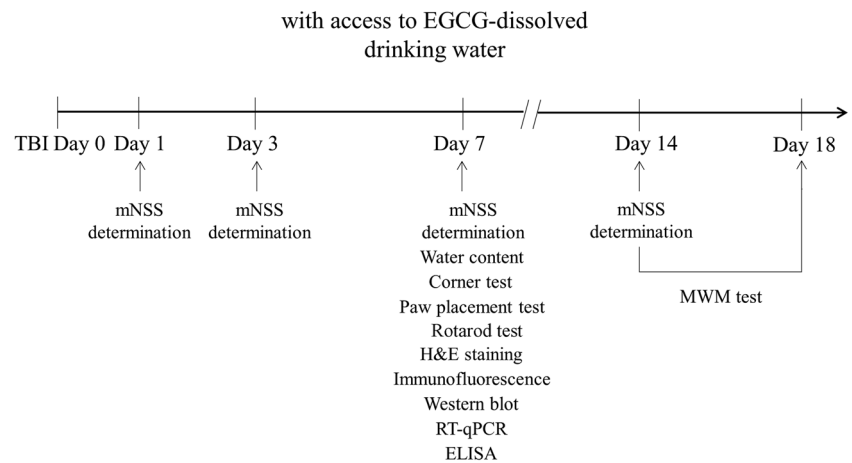
Corner test

To detect sensorimotor and postural asymmetries, corner test was carried out as described before (Leea et al. 2000; Yang et al. 2016; Zhang et al. 2002). A 30° angle of the corner was set up with two identical boards (30 × 20 cm dimension). Animals were placed halfway to the corner between two boards and facing the corner. When getting closer to the corner, both sides of the vibrissae were stimulated. Both right and left turns were recorded; the percentage of right turns from ten trials for each test was used to compare the CCI impairment. The turns that are not incorporated into a rearing movement were excluded.

Neurological severity score determination

Modified neurological severity score (mNSS) measures a variety of basic motor reflexes and coordination tasks to test for normal neurological function. The higher NSS indicates more severe impairment. A modified NSS (mNSS, the maximum score is 14) test was performed at 1, 3, 7, and 14 days after injury/sham procedures. The following tasks were included (Harun-Or-Rashid and Inman 2018): (1) forelimb flexion upon suspension by tail (score 0–3); (2) gait function when placed on the floor (0–3); (3) posture assessment by balance

Fig. 1 Schematic diagram of the experimental design. C57BL/6 mice underwent controlled cortical impact on the right cortex on day 0. Then, the mice were subjected to EGCG treatment until the end of the experiment. A group of tests was conducted to check the neurological function of the mice at the indicated time point. Besides, the brains were harvested post-injury for H&E staining, immunofluorescence, brain water content, and protein analysis. Sham mice were subjected to the same assays without undergoing brain injury

with access to EGCG-dissolved drinking water

TBI Day 0 Day 1   Day 3   Day 7   Day 14   Day 18

mNSS   mNSS   mNSS   mNSS
determination determination determination determination
                              Water content
                              Corner test
                              Paw placement test
                              Rotarod test
                              H&E staining
                              Immunofluorescence
                              Western blot
                              RT-qPCR
                              ELISA

MWM test

beam test (0–6); and (4) the pinna and corneal reflexes to evaluate reflex absence (0–2).

Rotarod test

The rotarod test provides a way to evaluate motor coordination and balance of the mice. Mice were trained in an accelerated protocol (rod rotating from 0 to 40 rpm) for 3 days (three sessions/day, 5 min/session) before CCI injury. Animals were subjected to the rotarod test on days 1, 3, 5, 7, and 14, and the latency to fall from the rotating rod was recorded.

Morris water maze

Spatial learning and memory were measured using the Morris water maze (MWM) for 5 consecutive days beginning at day 14 post-CCI injury, as described before (Ding et al. 2018). Briefly, the maze consists of a 100-cm-diameter water-tight pool and a 10-cm-diameter transparent platform. The water temperature was kept at 25 °C and filled to a depth of 1 cm above the platform. Various cues were hung on the surrounding walls to enable the mice to identify the location of the platform. The mice were subjected to 5 training days, each consisting of 4 trials, and the start positions were randomly changed each day. On each training day, the mice could swim up to 90 s in order to find the platform. If failed, they would be gently guided to the platform. Once on the platform, the mice could remain there for 30 s. The platform position will remain the same during the training sessions. On day 19 post-CCI procedure, a probe trial was conducted in the absence of the platform, and the mice could swim freely for 60 s. Swimming paths were recorded by a computerized video imaging analysis system (Jiliang Software Technology, Shanghai, China). Escape latency to find the platform (training sessions), time spent in the target quadrant, and platform crossing (probe trial) were reported.

Paw placement test

The mice were kept immobile in a horizontal position. Proprioceptive and tactile input was provided when the paw lost contact with the table surface and subsequently lightly contacting the paw with the edge of a table. The successful paw placement onto the edge of the table was recorded.

Immunofluorescence staining

For immunofluorescence staining, mice were perfused with saline and followed by 4% paraformaldehyde in 0.1 M phosphate-buffered saline (PBS, pH 7.4). After post-fixation in 4% paraformaldehyde and dehydration in 30% sucrose, the brains were sliced to 30-μm serial coronal free-floating sections. Sections were washed in 0.1 M PBS and blocked for 1 h at room temperature in 10% donkey serum blocking buffer (0.3% Triton X-100 in 0.1 M PBS). Sections were then incubated overnight at 4 °C with either one of the following primary antibodies: rabbit anti-NeuN antibody (1:50, Abcam, Cambridge, MA, USA), rabbit anti-Iba1 antibody (1:1000, Abcam, Cambridge, MA, USA), and rabbit anti-GFAP antibody (1:1000, Abcam, Cambridge, MA, USA) and diluted in blocking buffer. After primary antibody incubations, the sections were washed in 0.1 M PBS and incubated 2 h at room temperature with 1:300 AlexaFluor 647-conjugated donkey anti-rabbit antibodies (Abcam, Cambridge, MA). Sections were then incubated in PBS with DAPI solution (1:10,000, KeyGen Biotech, Nanjing, China) for counterstained nuclei.

Quantitative real-time polymerase chain reaction

Total RNA was extracted from CA1 regions of the hippocampus using RNeasy mini kit (Qiagen, Gaithersburg, MD) according to the manufacturer's instructions. In total, 0.6 μg of total RNA was used to synthesize complementary DNA (cDNA) with Super-Script IV first-strand synthesis kit (Invitrogen, Waltham, MA). Quantitative real-time

polymerase chain reaction (qRT-PCR) was performed with 10 μl SYBR Green PCR Master Mix (Applied Biosystems, Foster City, CA), 4 μl cDNA, and 0.3 μM of each primer for a specific target. Primers for real-time PCR were synthesized by Shang Hai City Liangtai Biotech (Shanghai, China). The amplification conditions consisted of 1 denaturation/activation cycle at 95 °C for 10 min, followed by 45 cycles at 95 °C for 15 s and 60 °C for 60 s. Serial dilutions of cDNA samples were used to obtain a standard curve. The relative amount of the target mRNA expression was calculated using SDS software (Applied Biosystems, HT7900, CA) and normalized with the housekeeping gene GAPDH.

Oxidative stress-related biochemical assays

Superoxide dismutase (SOD) assay kit (WST-1 method) and catalytic activity catalase (CAT) activity assay kit (visible light), malondialdehyde (MDA) assay kit (TBA method), and glutathione (GSH) assay kit (colorimetric method) were purchased from Nanjing Jiancheng Bioengineering Institute, Nanjing, China, and were performed according to the instructions of the manufacturer. Experiments were performed in triplicate.

ELISA

Tumor necrosis factor-α (TNF-α), interleukin-1β (IL-1β), and interleukin-6 (IL-6) levels in blood or brain homogenates were measured by ELISA according to the manufacturer's instructions (R&D Systems, Minneapolis, MN, USA). The sensitivity of the ELISA kits for TNF-α, IL-1β, and IL-6 is 7.21 ng/l, 4.8 ng/l, and 1.8 ng/l, respectively. Briefly, after preparing all reagents, standard dilutions, and samples as directed in the product insert, excess microplate strips were removed from the plate frame and then returned to the foil pouch containing the desiccant pack and reseal. Then 100 μl of assay diluent was added to each well, as well as 100 μl of standard, control or sample. The samples were covered with a plate sealer and incubated at room temperature for 2 h. After incubation, each well was aspirated and washed by repeating the process 3 times for a total of 4 washes. After washing, a biotin-conjugated secondary antibody was added to each well. Then, the samples were covered with a new plate sealer and incubated at room temperature for 2 h, followed by aspirating and washing 4 times. After washing, a 200-μl substrate solution was added to each well. Then, it was incubated at room temperature for 20 min. Finally, 50 μl of stop solution was added to each well. The samples were read at 450 nm within 30 min with wavelength correction to 540 nm or 570 nm.

Measurement of O_2 and H_2O_2

The lucigenin-enhanced chemiluminescence assay and manifestation of MitoSOX21 were used to determine the O_2-level, and an Amplex Red Hydrogen Peroxide/Peroxidase assay kit (Molecular Probe) was used to measure the H_2O_2 level in the hippocampus. Procedures were followed with the instructions provided by the manufacturer.

Western blot

The brain was exposed as reported above, and then the hippocampus was separated. The hippocampus lysate was obtained using a Tris-glycine SDS lysis buffer (Invitrogen). To determine the nuclear factor kappa-light-chain-enhancer of activated B cell (NF-κB)-p65 nuclear translocation, nuclear protein extracts were prepared using a nuclear extraction kit (Pierce, Rockford, IL), in accordance with the manufacturer's instructions. Protein concentration was determined with the bicinchoninic acid (BCA) assay kit (Thermo Fisher Scientific). Proteins were then separated by electrophoresis on 10–12% sodium dodecyl sulfate-polyacrylamide gel electrophoresis (SDS-PAGE) gel (Invitrogen) and transferred onto polyvinylidene difluoride (PVDF) membranes (Millipore, Burlington, MA). The membranes were blocked for 1 h in a blocking buffer containing 5% fat-free dry milk and incubated overnight with primary antibodies at 4 °C. Then, membranes were incubated with HRP-conjugated secondary antibody (1: 6000, KeyGen Biotech, Nanjing, China) for 1 h at room temperature. GAPDH or histone H3 was used as a loading control for whole-cell or nuclear samples, respectively. The proteins were detected using ECL chemiluminescence (Thermo Scientific, Waltham, WA).

Statistical analysis

Data were expressed as mean ± standard error of the mean (SEM). Statistical significance was determined using GraphPad Prism (version 6.0; GraphPad Software, San Diego, CA) by one-way ANOVA with Dunnett's least significant difference post hoc tests or two-way ANOVA analysis with a Bonferroni post hoc test. Differences were considered statistically significant at $p < 0.05$.

Results

EGCG improves neurological function in CCI-injured mice

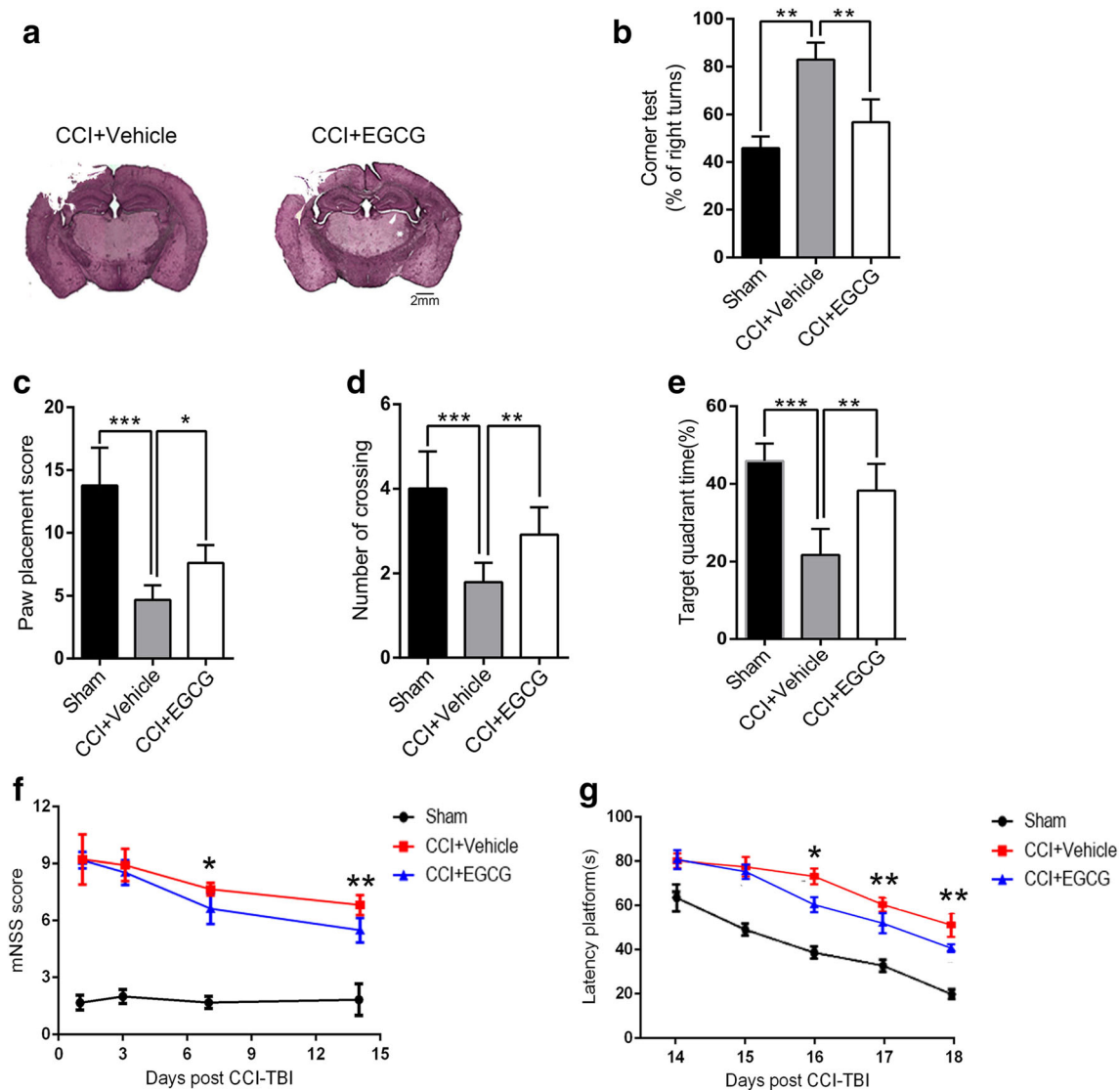Mayer's H&E staining was performed in CCI + vehicle and CCI + EGCG mice 7 days after CCI injury to examine the

Fig. 2 EGCG protects against controlled cortical impact-induced impairments of neurological function. a Representative Mayer's hematoxylin and eosin-stained brain sections obtained from vehicle and EGCG-treated mice at 7 days post-traumatic brain injury (TBI) (scale bar = 2 mm). b Corner test and c paw placement were determined at 7 days post-CCI. EGCG treatment increased the frequency of d platform crossing and e staying time in target quadrant in probe trial ($n = 6$ per group), measured by the Morris water maze test. ***$p < 0.001$, **$p < 0.01$, *$p < 0.05$. f The

severity of the tissue lesion. Figure 2A indicates an obvious cortex lesion in CCI + vehicle mice, which was alleviated by EGCG treatment.

Corner test, paw placement, and mNSS were performed 7 days or at the indicated time after CCI injury to further investigate the effects of EGCG on brain function recovery (Fig. 2b, d). In the corner test, the chance that mice turned right significantly increased in the CCI + vehicle group ($p < 0.01$) when compared with that in the sham group. However, EGCG administration brought it down to the level close to that of the sham group ($p < 0.01$;

motor, sensory, balance, and reflex functions were evaluated by modified neurological severity scores at 1, 3, 7, and 14 days after CCI procedure ($n = 10$ per group). **$p < 0.01$, *$p < 0.05$ of CCI + EGCG vs CCI + vehicle group. g The Morris water maze test was performed at days 14–18 post-injury to compare cognitive changes between EGCG-treated and CCI-operated animals ($n = 10$ per group). **$p < 0.01$, *$p < 0.05$ of CCI + EGCG vs CCI + vehicle group. Data are presented as means ± SEM

Fig. 2b). Paw placement data showed that mice in the CCI + vehicle group have less paw placement score compared with that in the sham group ($p < 0.001$). Treatment of EGCG partially yet significantly improved the paw placement score (Fig. 2c). The mNSS results revealed that mice in the EGCG-treated group had significantly lower scores at 1, 3, 7, and 14 days after CCI injury, compared with the CCI + vehicle group (Fig. 2d). The Morris water maze test was also performed in 5 consecutive days 2 weeks after CCI procedure. Mice in the EGCG group used remarkably shorter time to find the platform than

CCI-operated mice, starting from the third acquisition day and lasting to the last day tested (Fig. 2e). In the probe trial, mice in the CCI + vehicle group have less platform crossing numbers and spent less time in the target quadrant compared with sham mice ($p < 0.001$, $p < 0.001$) whereas EGCG treatment partially reversed the CCI-induced changes significantly (Fig. 2f, g).

EGCG reduces neuronal death and inflammation in mice after CCI injury

We hypothesized that EGCG could reduce neuronal death and inflammation in the hippocampus to ameliorate CCI-induced neurological deficits. Real-time PCR analysis showed a markedly decrease in the NeuN mRNA expression at 7 days post-CCI injury, which was completely restored by EGCG treatment (Fig. 3a, b). The Iba1 and GFAP gene expression was significantly increased as a consequence of CCI injury compared with the sham group. However, EGCG administration downregulated the CCI-induced Iba 1 and GFAP gene expression ($p < 0.001$, $p < 0.001$; Fig. 3a, b). Immunofluorescence staining in mice hippocampus also revealed similar results (Fig. 3c, d). Less NeuN-positive stained cells were shown in the CCI group compared with those in the sham group;

Iba1- and GFAP-positive staining were detected more as well upon CCI injury. EGCG treatment notably enhanced NeuN-positive cells and decreased Iba1 and GFAP staining compared with the CCI group (Fig. 3c, d).

EGCG reduces serum and brain inflammation and oxidative stress in mice after CCI injury

The inflammatory factors in blood and whole brain tissue were examined furthermore. CCI significantly increased both serum and brain TNF-α, IL-1β, and IL-6 level 24 h post-CCI; EGCG treatment markedly reduced CCI-induced inflammatory factor concentration (Fig. 4a, b). Oxidative stress was verified in the present CCI mice model. CCI enhanced O_2^-, H_2O_2, and MDA level and; decreased SOD, CAT activity, and GSH content in the brain 24 h after CCI ($p < 0.001$ on O_2^- level measurement, $p < 0.01$ on the rest); EGCG partially but significantly reversed these CCI-induced changes (Fig. 4c-h).

EGCG inhibits activation of NF-κB signaling pathway in mice after CCI injury

In order to investigate the underlying mechanisms involved in the anti-inflammation and anti-oxidative stress
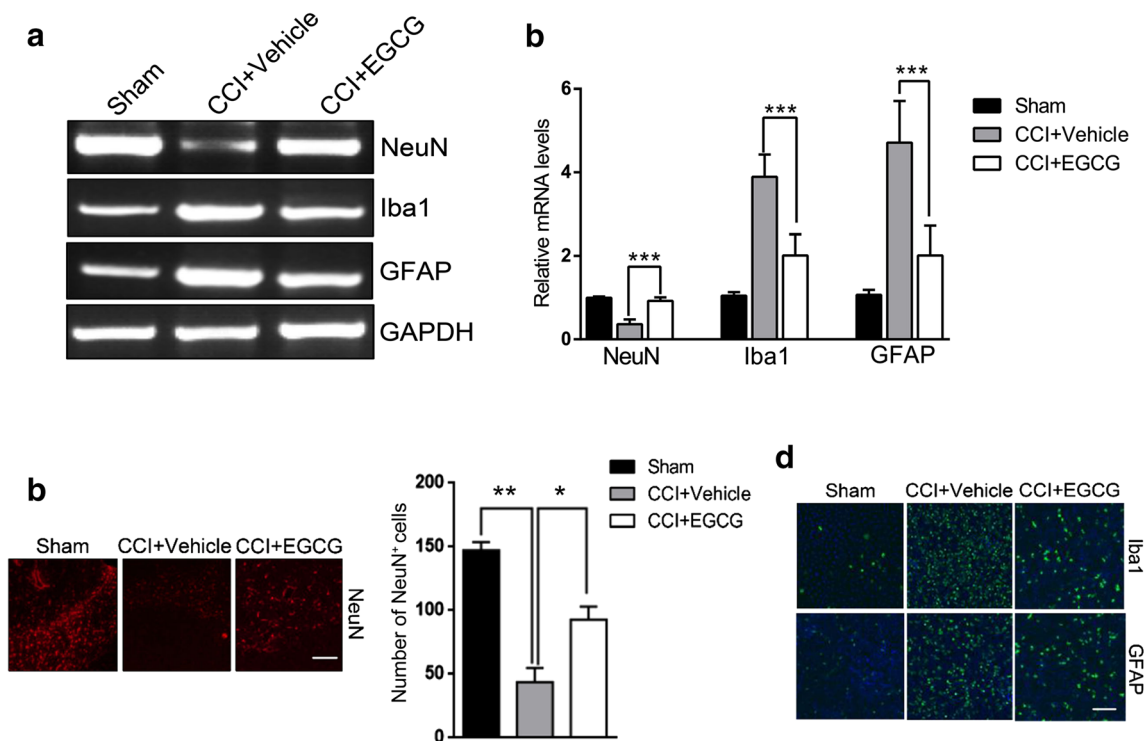

Fig. 3 EGCG reduced the activation of microglia and astrocytes. **a** Real-time PCR analysis of NeuN, Iba1, and GFAP in the hippocampus of mice at 7 days post-CCI-TBI ($n = 6$ per group). **b** Bar graph of the gene expression ($n = 6$ per group). **c** Immunofluorescence images and the statistical number of neurons (NeuN-positive) and **d** swollen (activated) microglia (Iba1-positive) and astrocytes (GFAP-positive) in the peri-traumatic area of brain sections of the sham, CCI + vehicle, and CCI + EGCG groups ($n = 6$ per group). Scale bar = 100 μm. Data are presented as means ± SEM. ***$p < 0.001$
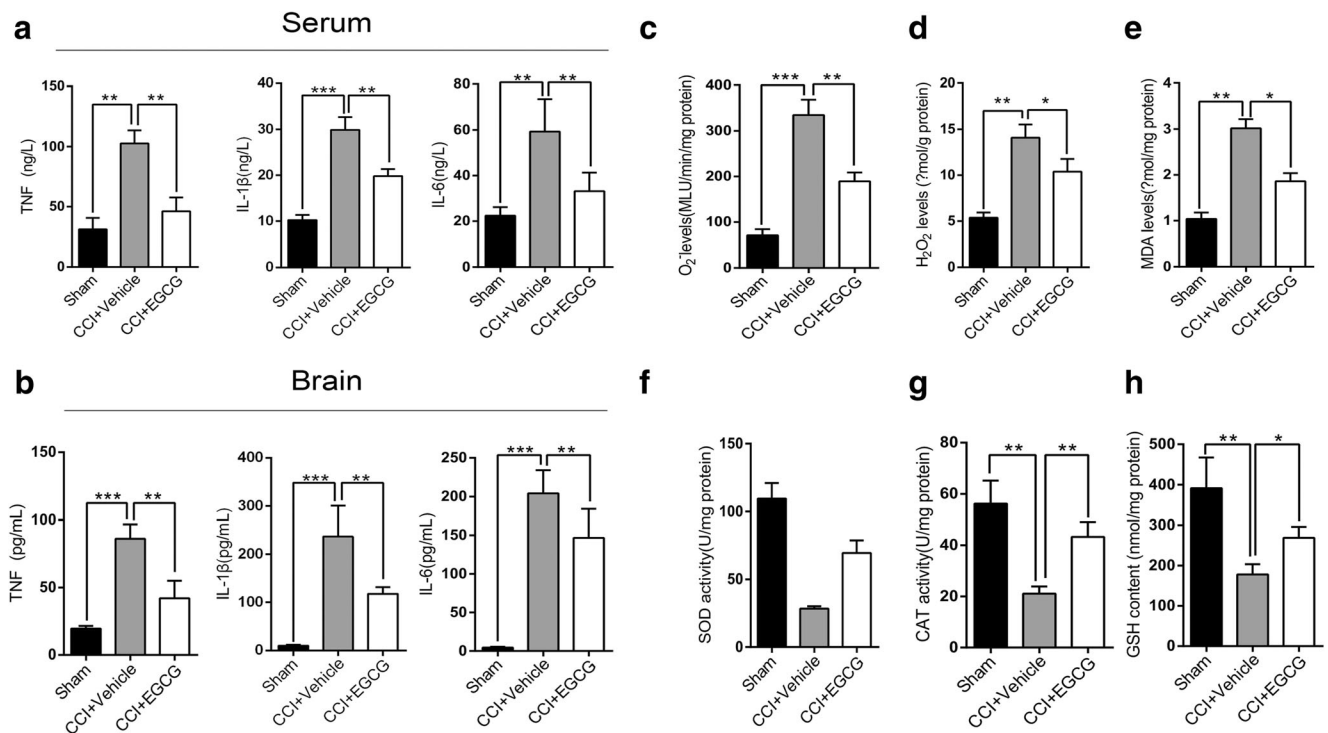
Fig. 4 EGCG reduces CCI-induced inflammation and oxidative stress in mice. **a** Serum and **b** brain pro-inflammatory cytokines, including TNF-α, IL-1β, and IL-6, were measured by ELISA. **c-h** The oxidative stress was determined by measuring O_2^-, H_2O_2, MDA levels, SOD, CAT activity, and GSH content in the hippocampus. Data are presented as means ± SEM, $n = 10$ per group. ***$p < 0.001$, **$p < 0.01$, *$p < 0.05$

effects of EGCG, the activation of the NF-κB signaling pathway in peri-traumatic brain tissue was detected 7 days after CCI procedure. CCI resulted in a prominent increase in phosphorylation of I kappa B kinase alpha /beta (IKKα/β), IκBα, and NF-κB p65 (Fig. 5a-d). EGCG markedly reduced IKKα/β and NF-κB p65 phosphorylation and completely suppressed IκB α phosphorylation (Fig. 5a-d).

EGCG prevents CCI-induced alterations of the activities of the AMPK signaling pathway in mice after CCI injury

The involvement of the AMPK pathway was assessed 7 days after CCI by Western blot. CCI introduced a significant decrease in the phosphorylation of AMPK (Fig. 6a, b). EGCG treatment partially prevented the change, presenting similar

Fig. 5 EGCG inhibits NF-κB activation in mice after CCI injury. **a** Representative Western blot results for phospho- and total IKKα/β, IκBα, and NF-κB p65 expression at 7 days post-CCI injury. **b-d** Bar graph of the protein quantification. Data are presented as means ± SEM, $n = 10$ per group. **$p < 0.01$, *$p < 0.05$
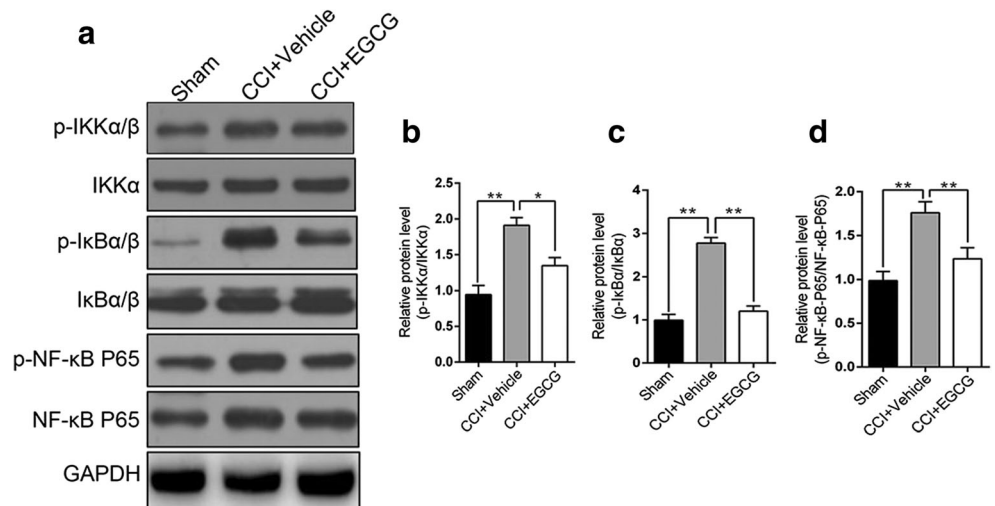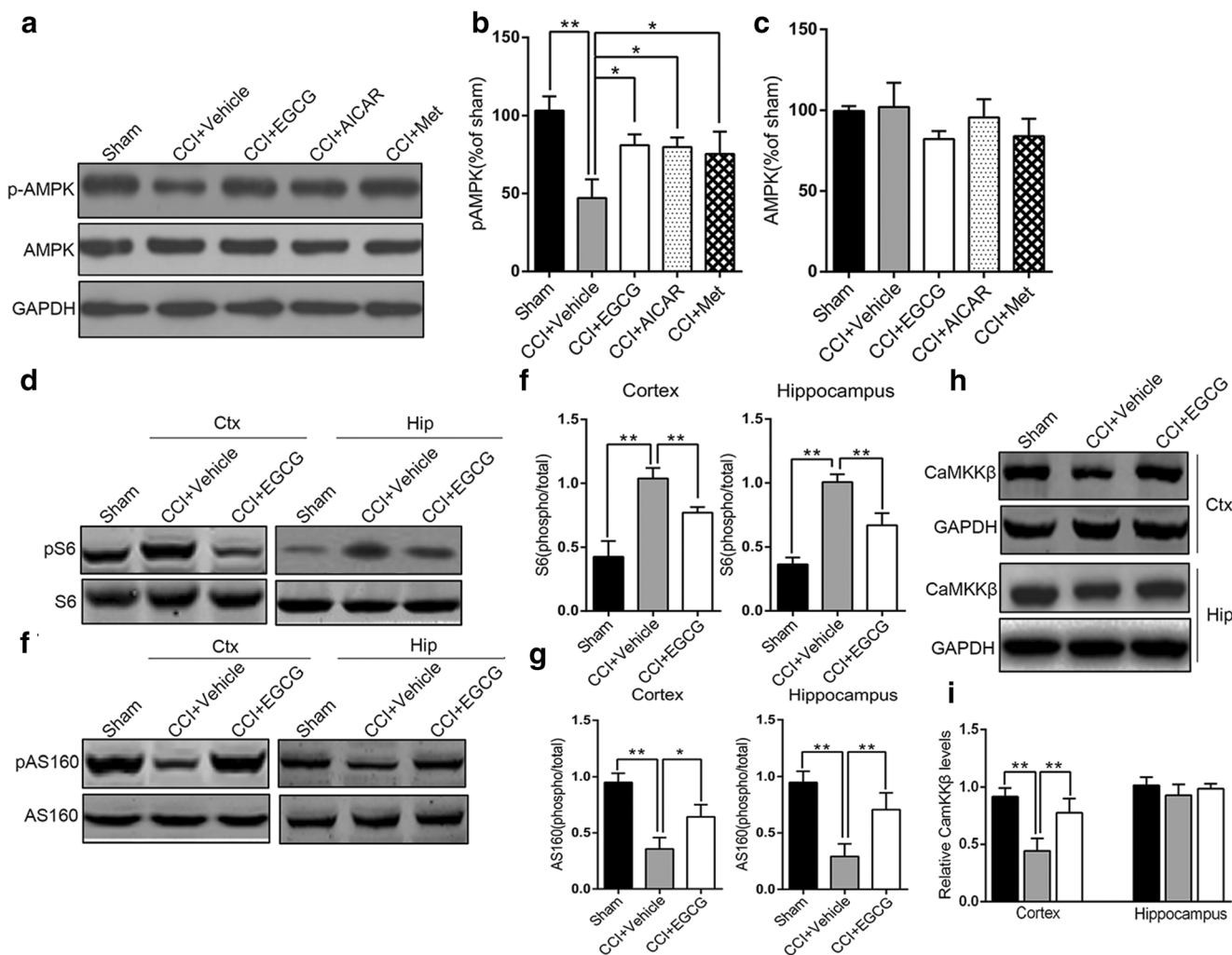
Fig. 6 EGCG prevents CCI-induced alterations in the phosphorylation of the AMPK pathway in mice after CCI injury. **a** Photographs of representative Western blots for phospho-AMPK, total AMPK, and GAPDH. **b, c** Bar graphs of the quantified protein levels. **d, e** Images of representative Western blots and summary data showing that S6 phosphorylation is increased in the ipsilateral cortex and hippocampus as a result of TBI, a direction of change consistent with a decrease in AMPK activity, which is reversed by EGCG treatment. **f, g** Images of representative Western blots and summary data showing that TBI reduces the phosphorylation of AS160 (phospho:total ratio) in both the ipsilateral cortex and hippocampus of injured rats, which can be reversed by EGCG treatment. **h, i** Images of representative Western blots for CaMKKß in the ipsilateral cortex and hippocampus from sham 7 days post-injury and EGCG-treated animals. Summary data showing that TBI significantly reduced CaMKKß level in the cortex, but not in the hippocampus, 7 days after injury, which can also be reversed by EGCG treatment. Data are presented as means ± SEM, $n = 10$ per group. **$p < 0.01$, *$p < 0.05$

effects as the AMPK activators AICAR and metformin ($p < 0.05$, $p < 0.05$, $p < 0.05$; Fig. 6a, b). The total AMPK expression remains at the same level at all the above circumstances (Fig. 6a, c). We then examined the phosphorylation of the AMPK substrates S6 and AS160 in both cortex and hippocampus. CCI injury significantly elevated the S6 phosphorylation and reduced the AS160 phosphorylation. EGCG treatment prevented the alterations under both brain regions ($p < 0.05$ on phosphor-AS160 in the cortex, $p < 0.01$ in the rest; Fig. 6d-g). The AMPK upstream protein kinase, Ca^{2+}/calmodulin-dependent protein kinase kinase-beta (CaMKKß), was examined too. The CaMKKß protein expression was downregulated by CCI injury only in the cortex ($p < 0.01$;

Fig. 6h, i), but not in the hippocampus. The CaMKKß protein level EGCG treatment inhibited the alteration of CaMKKß phosphorylation in the cortex and did not affect CaMKKß level in the hippocampus ($p < 0.01$; Fig. 6h, i).

AMPK is essential for EGCG effects on regulating CCI-induced inflammation and oxidative stress in mice

To further investigate the involvement of AMPK pathway in the mechanisms of EGCG effects, AMPKα1-knockout mice were used. Western blot results showed that the AMPK protein level was significantly decreased in the brain of
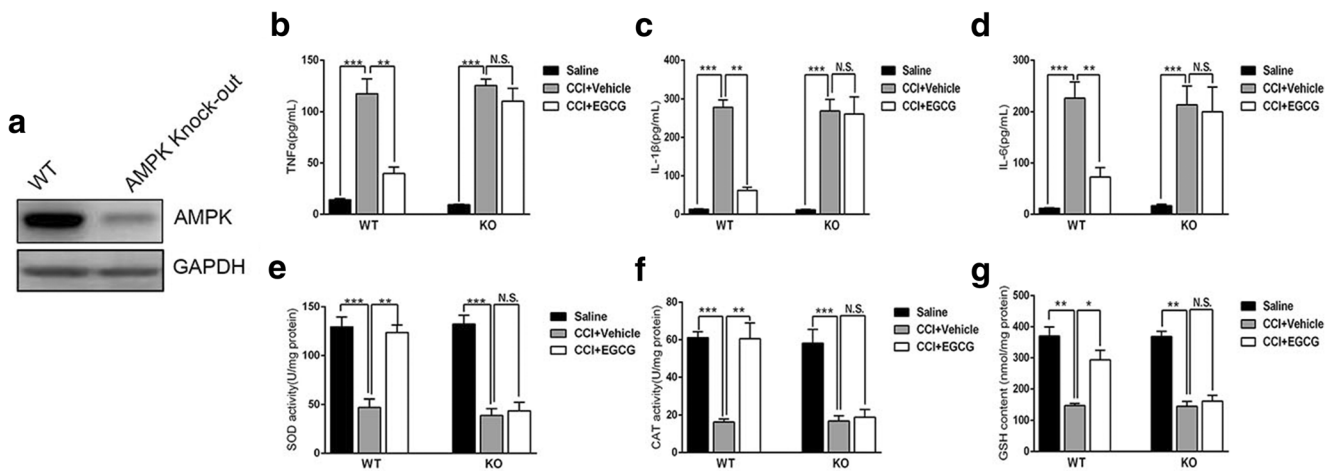
Fig. 7 AMPK is essential for EGCG effects on regulating CCI-induced inflammation and oxidative stress in mice. **a** Protein levels of AMPK in WT and AMPKα1-knockout mouse brain shown by Western blot picture. **b-d** TNF-α, IL-1β, and IL-6 levels in WT and KO mice brain after CCI and EGCG treatment ($n = 10$). **e-g** Analysis of SOD, CAT activity, and GSH content in the hippocampus following CCI injury. Data are presented as means ± SEM. ***$p < 0.001$, **$p < 0.01$, *$p < 0.05$. N.S., not significant

AMPKα1-knockout mice (Fig. 7a). While EGCG had the same effects on the CCI-induced increase in pro-inflammatory factors (TNF-α, IL-1β, and IL-6) and decrease in oxidative stress (SOD, CAT activity, and GSH content) level as detected in Fig. 4, the EGCG effects were completely diminished (Fig. 7b-g).

Discussion

The present study reveals that EGCG, an AMPK activator, has potent neuroprotective effects on CCI-induced neurological dysfunction in CCI, a mouse model of TBI (Osier and Dixon 2016; Romine et al. 2014). These effects are associated with anti-inflammation and anti-oxidation due to the suppression of CCI-induced NF-κB activation and AMPK de-activation.

Brain edema is a typical fatal pathological state in brain trauma, elevating intracranial pressure (ICP) due to an increase in the brain volume within the rigid enclosed skull (Jha et al. 2019; Michinaga and Koyama 2015). EGCG was reported to protect against spinal cord injury-induced spinal cord edema and TBI-induced brain edema in 72 h post-injury (Ge et al. 2013; Zhang et al. 2015). The elevation of ICP in the brain induces cerebral blood reduction, hypoxia, and high pressure on the cerebral tissue, which, in turn, causes impairment of neuronal function (Liu et al. 2018a). To further investigate the effects of EGCG on the recovery of brain tissue function, such as motor, sensory, balance, reflex functions, and spatial learning and memory, we performed corner test, paw placement test, mNSS, and Morris water maze test. As expected, EGCG treatment ameliorated CCI-induced neurological deficits. Cerebral edema mainly occurs as a result of secondary injury in CCI. Several mechanisms,

including neuronal excitotoxicity, the excessive inflammatory response to injury, and mitochondrial dysfunction, are involved (Jha et al. 2019; Michinaga and Koyama 2015). In our study, the real-time PCR analysis, immunofluorescence, and ELISA results revealed a decrease in the expression of a neuron marker NeuN after CCI injury, which could be restored by EGCG treatment. CCI procedure also increased the gene expression of Iba1 and GFAP, which are markers of activated microglia and astrocyte respectively. EGCG treatment after CCI attenuated the activation of microglia and astrocyte.

Among the mechanisms, inflammation and oxidation play key roles in inducing secondary injury (Jha et al. 2019; Michinaga and Koyama 2015). We therefore further tested the change of pro-inflammatory factors in serum and brain tissue. The results showed that the secretions of these pro-inflammatory factors were significantly increased in both serum and hippocampus CA1 region after CCI injury, while EGCG reduced these to a lower level, indicating that EGCG inhibits CCI-induced inflammation, which is corresponding to the findings on microglia and astrocyte activation. In addition, our assessment of hippocampus oxidative stress, as measured by O_2^-, H_2O_2, MDA levels, SOD, CAT activity, and GSH content, suggested that the CCI model in the present study succeeded to induce oxidative stress, and EGCG reversed this process.

The activation of the NF-κB pathway, by nuclear translocation of cytoplasmic complexed, plays a pivotal role in inflammation through its ability to induce transcription of pro-inflammatory genes and oxidative stress factors (Baldwin Jr. 1996; Bowie and O'Neill 2000; Tak and Firestein 2001). Recently, accumulating evidence has confirmed that the NF-κB pathway is partly responsible for the excessive inflammation in several models of neurological diseases (Jayakumar

et al. 2014; Wang et al. 2008). NF-κB remains inactive in the cytoplasm due to the binding to its endogenous inhibitory subunit, inhibitor kappa B (IκB) before inflammation simulation. Upon simulation, IκB is phosphorylated and degraded rapidly and then liberates and phosphorylated the NF-κB, facilitating its translocation to the nucleus and triggering the transcription of certain genes (Liu et al. 2018a). In our study, NF-κB p65, IκBα, and IKKα phosphorylation was found to be increased significantly after CCI injury. Furthermore, EGCG treatment attenuated this increase. NF-κB translocation was determined by Western blot using nucleus extract; we found that CCI injury resulted in an increase in nuclear NF-κB p65 levels, demonstrating the activation of NF-κB followed by CCI.

Abundant clinical studies and experimental data showed that TBI can cause prolonged inhibition of glucose metabolism and enhancement of inflammation and oxidation and affect brain function (Abdul-Muneer et al. 2015; Jalloh et al. 2015; Ley et al. 2012; Mendez 2017). AMPK, a serine/threonine kinase, is involved in all three events mentioned above (Mancini et al. 2017; Rabinovitch et al. 2017; Salminen et al. 2011). When activated, AMPK phosphorylates several substrates that lead to suppression of energy-consuming processes and enhancement of ATP-producing pathways and transcription of pro-inflammatory genes and oxidative stress factors. AMPK consists of three subunits: AMPKα, AMPKβ, and AMPKγ. AMP or ADP binds to the γ subunit when ATP is low, which results in a conformational change of the enzyme and then the residue Thr172 of the α unit is phosphorylated. Three kinases, liver kinase B1 (LKB1), transforming growth factor-activated kinase 1 (Tak1), and/or CaMKKβ, are responsible for the Thr172 phosphorylation (Krishan et al. 2015). Once phosphorylated on Thr172, AMPK activity increases by approximately 100-fold. Thus, targeting AMPK is one potential treatment strategy for TBI patients. In order to study the role of AMPK in the effects of EGCG, we first detected the phosphorylation level of Thr172 of AMPKα in mouse brain tissues. Western blot results showed that the phosphorylation level of Thr172 of AMPKα decreased after TBI treatment, and EGCG restored it. To further demonstrate that EGCG functions through AMPK, AMPK activator AICAR and metformin treatment groups were added. AICAR, metformin, and the combination of these two changed the phosphorylation of AMPK in the same way as EGCG. Next, we examined the phosphorylation levels of the AMPK substrate S6 (indirect) and AS160 (direct). EGCG was demonstrated to change the alterations at all circumstances. In view of the decreased phosphorylation level of AMPK after CCI injury, we also examined the upstream protein kinase of AMPK. Hill et al. (2016) reported a decrease in the level of CaMKKβ in the CCI-injured cerebral cortex; we also had similar findings and EGCG was proved to completely reverse the decrease.

While the AMPKα1 isoform represents the dominant catalytic activity of AMPK in rodent (Stapleton et al. 1996), an AMPKα1-knockout mouse model was generated to further verify the function of EGCG in TBI. The AMPKα protein expression was measured by Western blot and the result showed that it was substantially knocked out in the animals. Next, we found that AMPKα1 KO diminished the effect of EGCG on downregulating the levels of pro-inflammatory cytokines TNF-α, IL-1β, and IL-6, as well as upregulating the SOD, CAT, and GSH activity in the hippocampus in TBI-challenged mice.

There are several limitations to the current study. First, only one dose of EGCG was tested. It would be nice to include more doses in future studies. Second, it is preferred to compare the effects of ECGG with other well-known drugs. Third, other kinds of TBI model could be employed to strengthen the conclusions.

In summary, the current work demonstrates that EGCG regulates inflammation and oxidative stress through the AMPK pathway and ameliorates CCI-induce neurological deficits, indicating that EGCG is a potent neuro-protectant in CCI injury.

Conclusion

Our investigation demonstrates that EGCG protects against CCI-induced neurological functions through the activation of the AMPK pathway in mice. These results suggest that EGCG might be a promising therapeutic intervention preventing locomotor and cognitive impairment after traumatic brain injury.

Authors' contributions Yinyin Wu and Jing Cui conceptualized the study and conducted the literature review for all databases. Jing Cui performed all statistical analyses. Yinyin Wu drafted the paper.

Compliance with ethical standards

Conflict of interest The authors declare that they have no conflict of interest.

References

Abdul-Muneer PM, Chandra N, Haorah J (2015) Interactions of oxidative stress and neurovascular inflammation in the pathogenesis of traumatic brain injury. Mol Neurobiol 51:966–979. https://doi.org/10.1007/s12035-014-8752-3

Baldwin AS Jr (1996) The NF-kappa B and I kappa B proteins: new discoveries and insights. Annu Rev Immunol 14:649–683. https://doi.org/10.1146/annurev.immunol.14.1.649

Bowie A, O'Neill LA (2000) Oxidative stress and nuclear factor-kappaB activation: a reassessment of the evidence in the light of recent discoveries. Biochem Pharmacol 59:13–23

Briones TL, Woods J, Rogozinska M (2013) Decreased neuroinflammation and increased brain energy homeostasis following environmental enrichment after mild TBI is associated with improvement in cognitive function. Acta Neuropathol Commun:1

Chu C, Deng J, Man Y, Qu Y (2017) Green tea extracts epigallocatechin-3-gallate for different treatments. Biomed Res Int 2017:5615647. https://doi.org/10.1155/2017/5615647

Ding L, Gao X, Hu J, Yu S (2018) (-)Epigallocatechin3gallate attenuates anesthesiainduced memory deficit in young mice via modulation of nitric oxide expression. Mol Med Rep 18:4813–4820. https://doi.org/10.3892/mmr.2018.9548

Ehrnhoefer DE et al (2008) EGCG redirects amyloidogenic polypeptides into unstructured, off-pathway oligomers. Nat Struct Mol Biol 15:558–566. https://doi.org/10.1038/nsmb.1437

Ge R, Zhu Y, Diao Y, Tao L, Yuan W, Xiong XC (2013) Anti-edema effect of epigallocatechin gallate on spinal cord injury in rats. Brain Res 1527:40–46. https://doi.org/10.1016/j.brainres.2013.06.009

Harun-Or-Rashid M, Inman DM (2018) Reduced AMPK activation and increased HCAR activation drive anti-inflammatory response and neuroprotection in glaucoma. J Neuroinflammation 15:313. https://doi.org/10.1186/s12974-018-1346-7

Hill JL, Kobori N, Zhao J, Rozas NS, Hylin MJ, Moore AN, Dash PK (2016) Traumatic brain injury decreases AMP-activated protein kinase activity and pharmacological enhancement of its activity improves cognitive outcome. J Neurochem 139:106–119. https://doi.org/10.1111/jnc.13726

Ide K, Matsuoka N, Yamada H, Furushima D, Kawakami K (2018) Effects of tea catechins on Alzheimer's disease: recent updates and perspectives. Molecules:23. https://doi.org/10.3390/molecules23092357

Ikeda I (2008) Multifunctional effects of green tea catechins on prevention of the metabolic syndrome. Asia Pac J Clin Nutr 17(Suppl 1):273–274

Itoh T, Imano M, Nishida S, Tsubaki M, Mizuguchi N, Hashimoto S, Ito A, Satou T (2012) (−)-Epigallocatechin-3-gallate increases the number of neural stem cells around the damaged area after rat traumatic brain injury. J Neural Transm (Vienna) 119:877–890. https://doi.org/10.1007/s00702-011-0764-9

Jalloh I, Carpenter KL, Helmy A, Carpenter TA, Menon DK, Hutchinson PJ (2015) Glucose metabolism following human traumatic brain injury: methods of assessment and pathophysiological findings. Metab Brain Dis 30:615–632. https://doi.org/10.1007/s11011-014-9628-y

Jayakumar AR, Tong XY, Ruiz-Cordero R, Bregy A, Bethea JR, Bramlett HM, Norenberg MD (2014) Activation of NF-kappaB mediates astrocyte swelling and brain edema in traumatic brain injury. J Neurotrauma 31:1249–1257. https://doi.org/10.1089/neu.2013.3169

Jha RM, Kochanek PM, Simard JM (2019) Pathophysiology and treatment of cerebral edema in traumatic brain injury. Neuropharmacology 145:230–246. https://doi.org/10.1016/j.neuropharm.2018.08.004

Kaur P, Sharma S (2018) Recent advances in pathophysiology of traumatic brain injury. Curr Neuropharmacol 16:1224–1238. https://doi.org/10.2174/1570159X15666170613083606

Khan M, Shunmugavel A, Dhammu TS, Khan H, Singh I, Singh AK (2018) Combined treatment with GSNO and CAPE accelerates functional recovery via additive antioxidant activities in a mouse model of TBI. J Neurosci Res 96:1900–1913. https://doi.org/10.1002/jnr.24279

Kondo T, Ohta T, Igura K, Hara Y, Kaji K (2002) Tea catechins inhibit angiogenesis in vitro, measured by human endothelial cell growth, migration and tube formation, through inhibition of VEGF receptor binding. Cancer Lett 180:139–144

Krishan S, Richardson DR, Sahni S (2015) Adenosine monophosphate-activated kinase and its key role in catabolism: structure, regulation, biological activity, and pharmacological activation. Mol Pharmacol 87:363–377. https://doi.org/10.1124/mol.114.095810

Lecumberri E, Dupertuis YM, Miralbell R, Pichard C (2013) Green tea polyphenol epigallocatechin-3-gallate (EGCG) as adjuvant in cancer therapy. Clin Nutr 32:894–903. https://doi.org/10.1016/j.clnu.2013.03.008

Leea S, Suhb S, Kimc S (2000) Protective effects of the green tea polyphenol (−)-epigallocatechin gallate against hippocampal neuronal damage after transient global ischemia in gerbils.Pdf. Neurosci Lett 287:191–194

Ley EJ, Clond MA, Bukur M, Park R, Chervonski M, Dagliyan G, Margulies DR, Lyden PD, Conti PS, Salim A (2012) Beta-adrenergic receptor inhibition affects cerebral glucose metabolism, motor performance, and inflammatory response after traumatic brain injury. J Trauma Acute Care Surg 73:33–40. https://doi.org/10.1097/TA.0b013e31825a769b

Li F et al (2018) Perspectives on the recent developments with green tea polyphenols in drug discovery. Expert Opin Drug Discov 13:643–660. https://doi.org/10.1080/17460441.2018.1465923

Liu YL et al (2018a) Adjudin attenuates cerebral edema and improves neurological function in mice with experimental traumatic brain injury. J Neurotrauma 35:2850–2860. https://doi.org/10.1089/neu.2017.5397

Liu ZM et al (2018b) RIP3 deficiency protects against traumatic brain injury (TBI) through suppressing oxidative stress, inflammation and apoptosis: dependent on AMPK pathway. Biochem Biophys Res Commun 499:112–119. https://doi.org/10.1016/j.bbrc.2018.02.150

Loane DJ, Faden AI (2010) Neuroprotection for traumatic brain injury: translational challenges and emerging therapeutic strategies. Trends Pharmacol Sci 31:596–604. https://doi.org/10.1016/j.tips.2010.09.005

Maas A, Menon D, Adelson P et al (2017) Traumatic brain injury: integrated approaches to improve prevention, clinical care, and research. Lancet Neurol 16:987–1048. https://doi.org/10.1016/S1474-4422(17)30371-X

Mancini SJ et al (2017) Activation of AMP-activated protein kinase rapidly suppresses multiple pro-inflammatory pathways in adipocytes including IL-1 receptor-associated kinase-4 phosphorylation. Mol Cell Endocrinol 440:44–56. https://doi.org/10.1016/j.mce.2016.11.010

Mendez MF (2017) What is the relationship of traumatic brain injury to dementia? J Alzheimers Dis 57:667–681. https://doi.org/10.3233/JAD-161002

Meng Q, Velalar CN, Ruan R (2008) Regulating the age-related oxidative damage, mitochondrial integrity, and antioxidative enzyme activity in Fischer 344 rats by supplementation of the antioxidant epigallocatechin-3-gallate. Rejuvenation Res 11:649–660. https://doi.org/10.1089/rej.2007.0645

Michinaga S, Koyama Y (2015) Pathogenesis of brain edema and investigation into anti-edema drugs. Int J Mol Sci 16:9949–9975. https://doi.org/10.3390/ijms16059949

Nagai K, Jiang MH, Hada J, Nagata T, Yajima Y, Yamamoto S, Nishizaki T (2002) (−)-Epigallocatechin gallate protects against NO stress-induced neuronal damage after ischemia by acting as an anti-oxidant. Brain Res 956:319–322

Osier ND, Dixon CE (2016) The controlled cortical impact model: applications, Considerations for researchers, and future directions. Front Neurol 7:134. https://doi.org/10.3389/fneur.2016.00134

Pearn ML et al (2017) Pathophysiology associated with traumatic brain injury: current treatments and potential novel therapeutics cell. Mol Neurobiol 37:571–585. https://doi.org/10.1007/s10571-016-0400-1

Pushkarna A, Bhatoe HS, Sudambrekar SM (2010) Head injuries. Med J Armed Forces India 66:321–324. https://doi.org/10.1016/S0377-1237(10)80008-5

Rabinovitch RC et al (2017) AMPK maintains cellular metabolic homeostasis through regulation of mitochondrial reactive oxygen species. Cell Rep 21:1–9. https://doi.org/10.1016/j.celrep.2017.09.026

Romine J, Gao X, Chen J (2014) Controlled cortical impact model for traumatic brain injury. J Vis Exp:e51781. https://doi.org/10.3791/51781

Salminen A, Hyttinen JM, Kaarniranta K (2011) AMP-activated protein kinase inhibits NF-kappaB signaling and inflammation: impact on healthspan and lifespan. J Mol Med (Berl) 89:667–676. https://doi.org/10.1007/s00109-011-0748-0

Scheff SW, Ansari MA (2017) Natural Compounds as a therapeutic intervention following traumatic brain injury: the role of phytochemicals. J Neurotrauma 34:1491–1510. https://doi.org/10.1089/neu.2016.4718

Stapleton D, Mitchelhill KI, Gao G, Widmer J, Michell BJ, Teh T, House CM, Fernandez CS, Cox T, Witters LA, Kemp BE (1996) Mammalian AMP-activated protein kinase subfamily. J Biol Chem 271:611–614. https://doi.org/10.1074/jbc.271.2.611

Tak PP, Firestein GS (2001) NF-kappaB: a key role in inflammatory diseases. J Clin Invest 107:7–11. https://doi.org/10.1172/JCI11830

Tang FY, Nguyen N, Meydani M (2003) Green tea catechins inhibit VEGF-induced angiogenesis in vitro through suppression of VE-cadherin phosphorylation and inactivation of Akt molecule. Int J Cancer 106:871–878. https://doi.org/10.1002/ijc.11325

Tedeschi E, Menegazzi M, Yao Y, Suzuki H, Forstermann U, Kleinert H (2004) Green tea inhibits human inducible nitric-oxide synthase expression by down-regulating signal transducer and activator of transcription-1alpha activation. Mol Pharmacol 65:111–120. https://doi.org/10.1124/mol.65.1.111

Wang ZF, Wang J, Zhang HY, Tang XC (2008) Huperzine A exhibits anti-inflammatory and neuroprotective effects in a rat model of transient focal cerebral ischemia. J Neurochem 106:1594–1603. https://doi.org/10.1111/j.1471-4159.2008.05504.x

Xiong Y, Mahmood A, Chopp M (2013) Animal models of traumatic brain injury. Nat Rev Neurosci 14:128–142. https://doi.org/10.1038/nrn3407

Yang L, Guo Y, Wen D, Yang L, Chen Y, Zhang G, Fan Z (2016) Bone fracture enhances trauma brain injury. Scand J Immunol 83:26–32. https://doi.org/10.1111/sji.12393

Zhang L, Schallert T, Zhang ZG, Jiang Q, Arniego P, Li Q, Lu M, Chopp M (2002) A test for detecting long-term sensorimotor dysfunction in the mouse after focal cerebral ischemia. J Neurosci Methods 117:207–214

Zhang B, Wang B, Cao S, Wang Y (2015) Epigallocatechin-3-gallate (EGCG) attenuates traumatic brain injury by inhibition of edema formation and oxidative stress. Korean J Physiol Pharmacol 19:491–497. https://doi.org/10.4196/kjpp.2015.19.6.491